Supporting Information for

Cobalt Doped β-Molybdenum Carbide Nanoparticles Encapsulated within Nitrogen-Doped Carbon for Oxygen Evolution

Xinyang Zhu[a,b], Xueping Zhang[a,c], Liang Huang[a,b], Yongqin Liu[a], He Zhang[a,b] and Shaojun Dong[*,a,b]

[a]State Key Laboratory of Electroanalytical Chemistry, Changchun Institute of Applied Chemistry, Chinese Academy of Science, Changchun, Jilin 130022, P. R. China
[b]University of Science and Technology of China, Hefei, Anhui 230026, P. R. China

E-mail: dongsj@ciac.ac.cn.

Experimental section

Materials

Zinc nitrate hexahydrate ($Zn(NO)_2 \cdot 6H_2O$) and cobalt nitrate hexahydrate ($Co(NO)_2 \cdot 6H_2O$) were purchased from Xilong Chemical Engineering Co.. 2-methylimidazole was obtained from Aladdin Industrial Co.. Bis(acetylacetonato)dioxomolybdenum (VI) ($MoO_2(acac)_2$) was bought from Meryer Chemical Technology Co., Ltd.. Methanol and N, N-dimethylformamide (DMF) were purchased from Beijing Chemical Co.. Nafion (5.0 wt%) was purchased from Sigma-Aldrich. In the experiment, all chemical agents were used as received without further purification.

Synthesis of Co_n-β-Mo_2C@NC

Synthesis of ZIF ZIF-8 was synthesized following the method previously reported[1]. Three samples with different Co/Zn mole ratios (Co/Zn=0.2, 0.1 and 0.05) were prepared, dubbed as 0.2-ZIF, 0.1-ZIF and 0.05-ZIF, respectively. Typically, 1.68 g $Zn(NO_3)_2 \cdot 6H_2O$ were dissolved in 40 mL methanol with 0.32 g, 0.16 g and 0.08 g $Co(NO_3)_2 \cdot 6H_2O$ at room temperature, respectively. 3.7 g 2-methylimidazole were dissolved in 40 mL methanol at room temperature, respectively. Then the mixture solution of $Zn(NO_3)_2 \cdot 6H_2O$ and $Co(NO_3)_2 \cdot 6H_2O$ was poured into methanol solution of 2-methylimidazole under vigorous stirring for 24 h, respectively. The reaction products were collected through centrifugation, and washed by methanol for three times, then dried at 60 °C for 12 h. Morphology of the ZIFs was shown in the Fig.S1.

Synthesis of Co_n-β-Mo_2C@NC Firstly, 0.02 g $MoO_2(acac)_2$ were dissolved in 200 μL DMF, respectively. Afterwards, 80 mg 0.2-ZIF, 0.1-ZIF and 0.05-ZIF were obtained, keeping in three 5 mL volume centrifuge tubes. DMF solution of $MoO_2(acac)_2$ was dropped into the three centrifuge tubes, respectively, then the mixtures were vibrated with mixer for 5 minutes. After that, mixtures were put into vacuum drying oven at 60 °C for 12 h. Subsequently, dried products were ground to fine powder and put into porcelain boats, which were then calcinated at 900 °C for 3 h with a heating rate of 3 °C min^{-1} in N_2 atmosphere. The samples as-obtained were

dubbed as Co_n-β-Mo_2C@NC.

Characterization

X-ray diffraction (XRD) data were obtained from a D8 ADVANCE (Bruker, Germany) X-ray diffractometer with Cu Kα radiation (λ =1.5406 Å). Scanning electron microscopy (SEM) measurements were carried out on a PHILIPS XL-30 field-emission scanning electron microscope with an accelerating voltage of 10 kV. Transmission electron microscopy (TEM) experiments were performed on a TECNAI F20 field-emission transmission electron microscope with an accelerating voltage of 200 kV. X-ray photoelectron spectra (XPS) were acquired on an ESCALAB-MKII X-ray photoelectron spectrometer with an excitation source of Al Kα radiation. Raman spectra were recorded on a LabRAM HR800 confocal Raman microscope (Horiba Jobin Yvon) with a laser excitation of 633 nm and power of 5 %. Nitrogen adsorption/desorption analysis was performed at 77.15 K on the AutosorbStation1 (Quantachrome, USA). Before measurement, the samples were degassed at 150 °C under vacuum for 12 h.

Electrochemical measurements

The OER measurements were performed in a three-electrodes system on a CHI832c electrochemical workstation with a Model RRDE-3A Apparatus (BAS Japan) at room temperature. A Pt wire and Ag/AgCl (saturated KCl) electrodes were used as counter electrode and reference electrode, respectively. To prepare working electrode, 2 mg sample was dissolved 1 mL in ethanol containing 0.12 wt.% Nafion solution under sonication. After that, 18 μL of the mixture was dropped onto the glassy carbon of RDE with a diameter of 4 mm, then left it dry in air. The catalyst loading amount was about 0.28 mg/cm^2 on the working electrode surface. Linear sweep voltammetry (LSV) experiments were performed at a scan rate of 5 mV/s and a rotating speed of 1600 rpm with a correction of 95% iR-compensation in 1.0 M KOH solution which was purged with O_2 for 15 minutes. The potential measured versus Ag/AgCl (saturated KCl) electrode was converted to versus reversible hydrogen electrode (RHE) according to $E_{vs.RHE} = E_{vs.Ag/AgCl} + E_{Ag/AgCl}^{\Theta} + 0.0592pH_2$. The overpotential (η) of the reaction can be obtained according to $\eta = E_{vs.RHE} - 1.23\,V$. Current density (J) was normalized to the

geometrical area of RDE. Electrochemical impendence spectroscopy (EIS) measurements were performed at an overpotential of 600 mV *vs.* RHE from 1 MHz to 0.1 Hz with an amplitude of 5 mV.

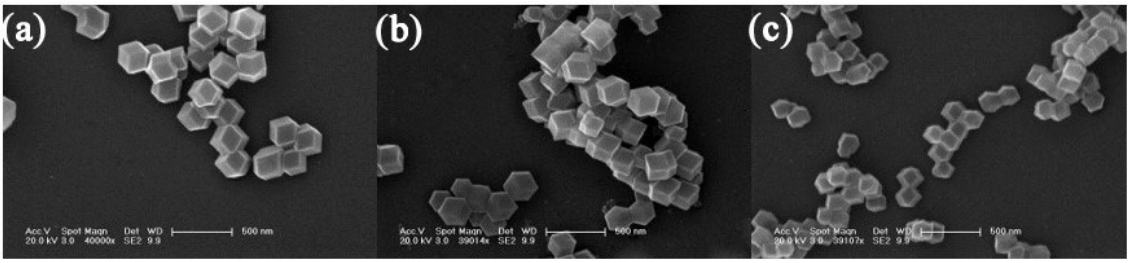

Figure. S1 Scanning electron microscopy (SEM) images of bimetallic ZIFs with different Zn/Co mole ratios, (a) 5:1, (b) 10:1, (c) 20:1.

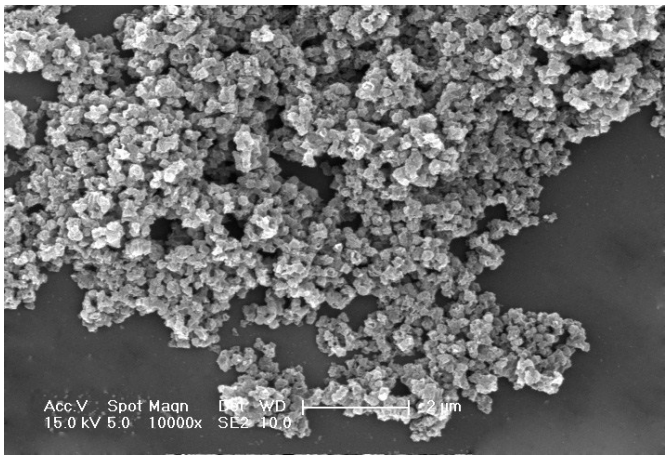

Figure. S2 Scanning electron microscopy (SEM) image of $Co_{0.1}$-β-Mo_2C@NC.

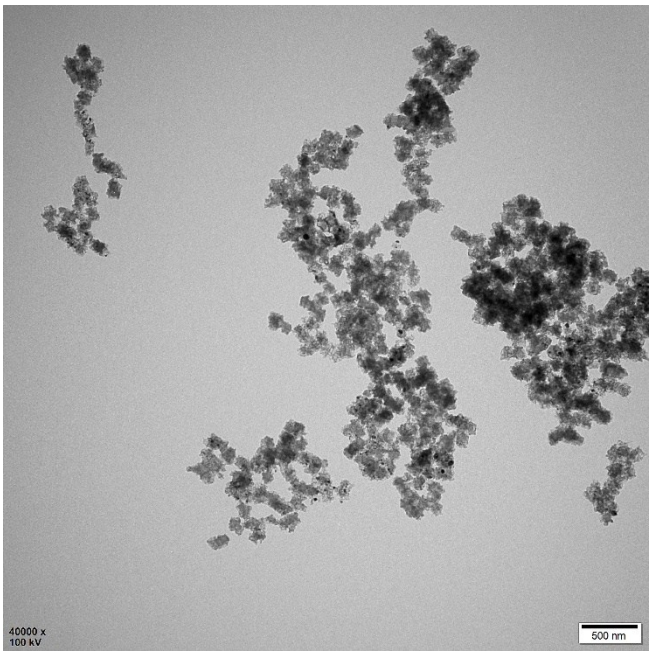

Figure. S3 Low magnification TEM image of $Co_{0.1}$-β-Mo_2C@NC.

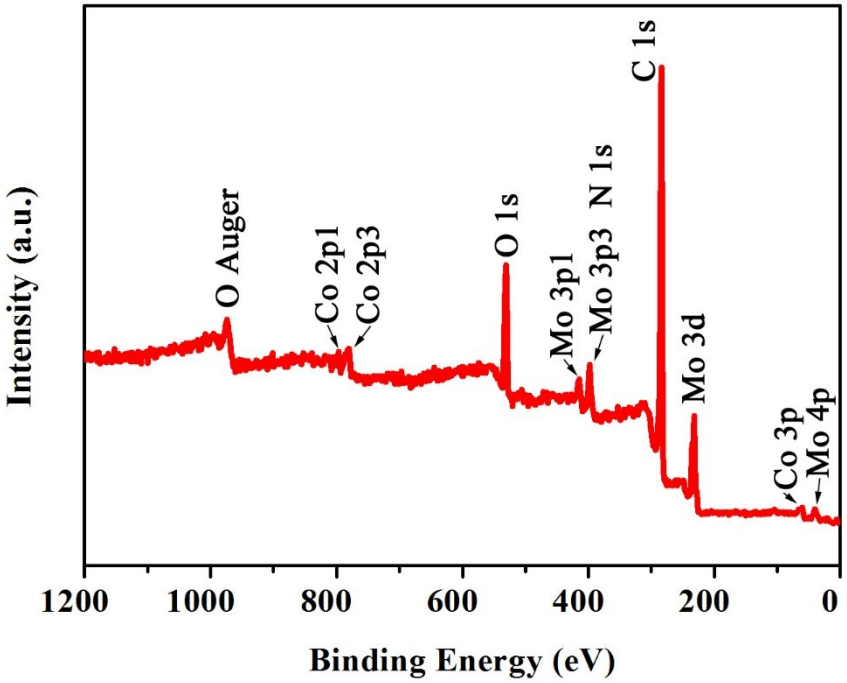

Figure. S4 XPS survey spectrum of $Co_{0.1}$-β-Mo_2C@NC.

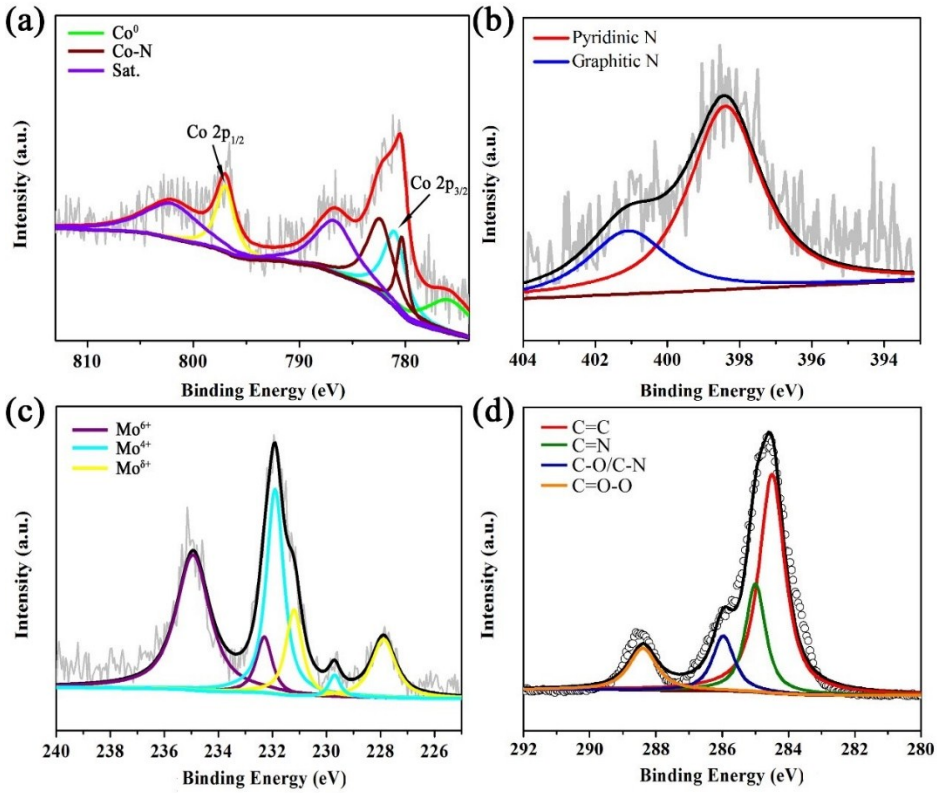

Figure. S5 XPS spectra of $Co_{0.1}$-β-Mo_2C@NC, (a) Co, (b) N, (c) Mo and (d) C.

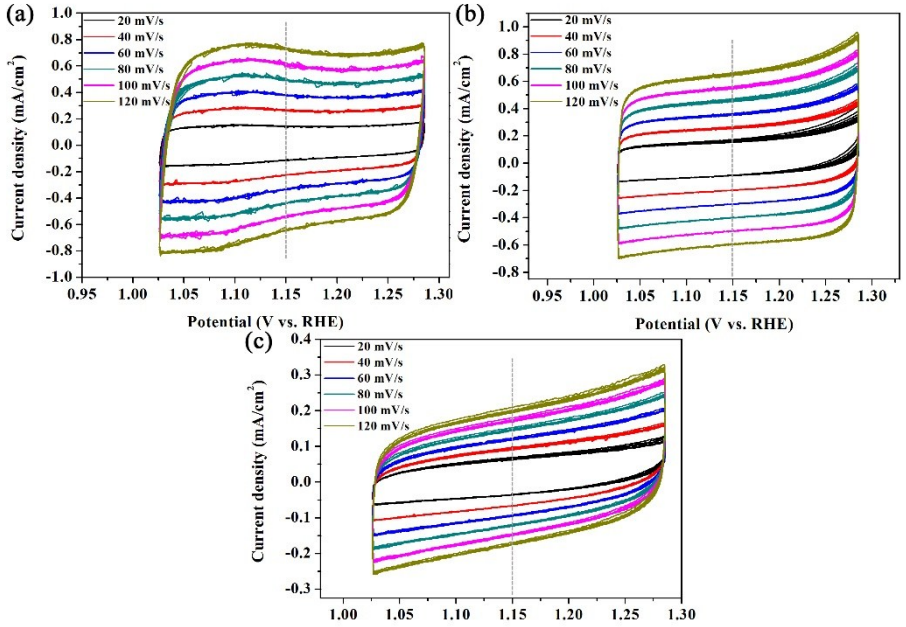

Figure. S6 Cyclic voltammograms of (a) $Co_{0.2}$-β-Mo_2C@NC, (b) $Co_{0.1}$-β-Mo_2C@NC, (c) $Co_{0.05}$-β-Mo_2C@NC with various scan rates in 1.0 M KOH.

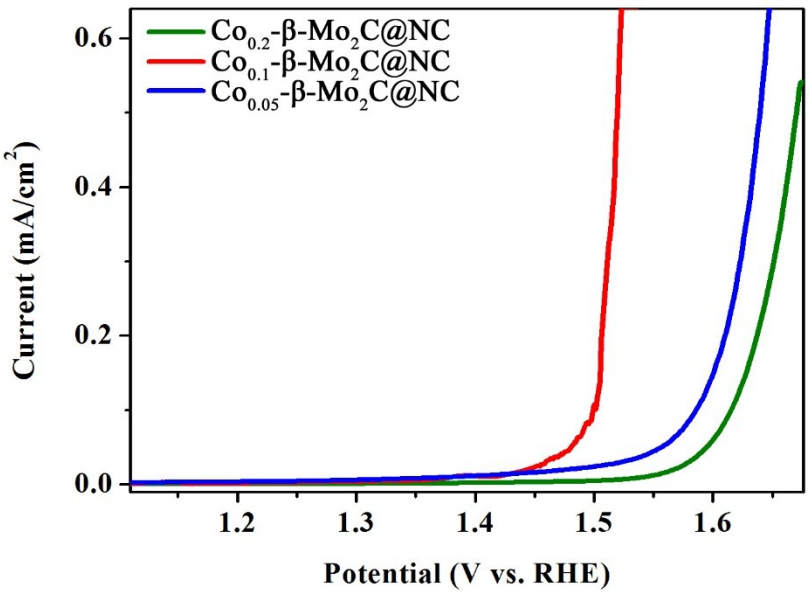

Figure. S7 The specific OER activity calculated by normalizing the current based on the corresponding ECSA of Co_n-β-Mo_2C@NC in 1 M KOH.

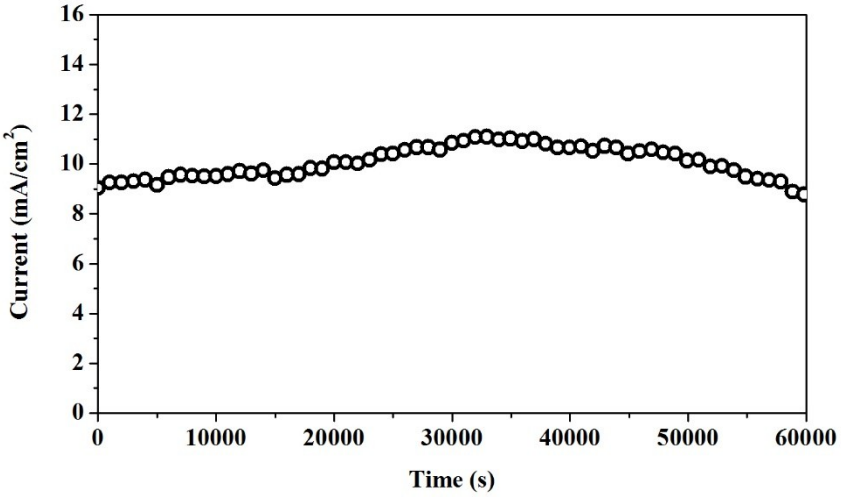

Figure. S8 I-t plot of $Co_{0.1}$-β-Mo_2C@NC at a controlled potential of 1.49 V.

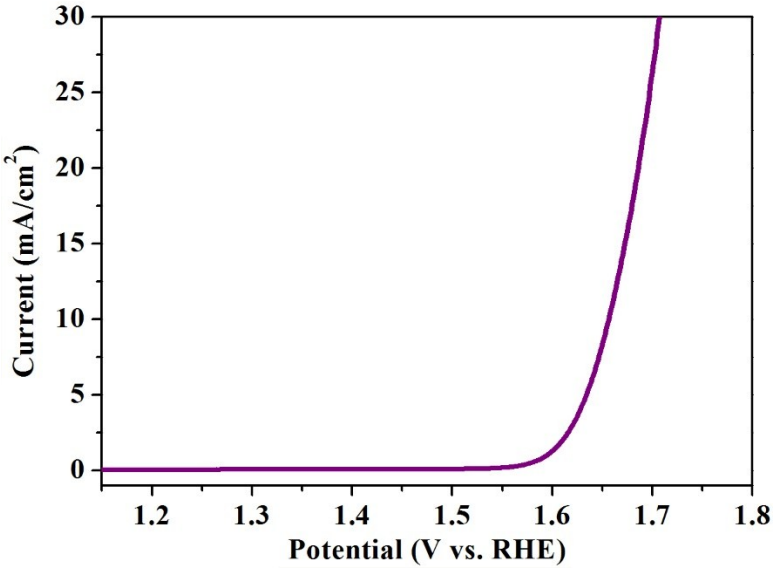

Figure. S9 LSV curves of $Co_{0.1}$@NC after iR-compensation in 1 M KOH aqueous solution at a scan rate of 5 mV/s and a rotating speed of 1600 rpm.

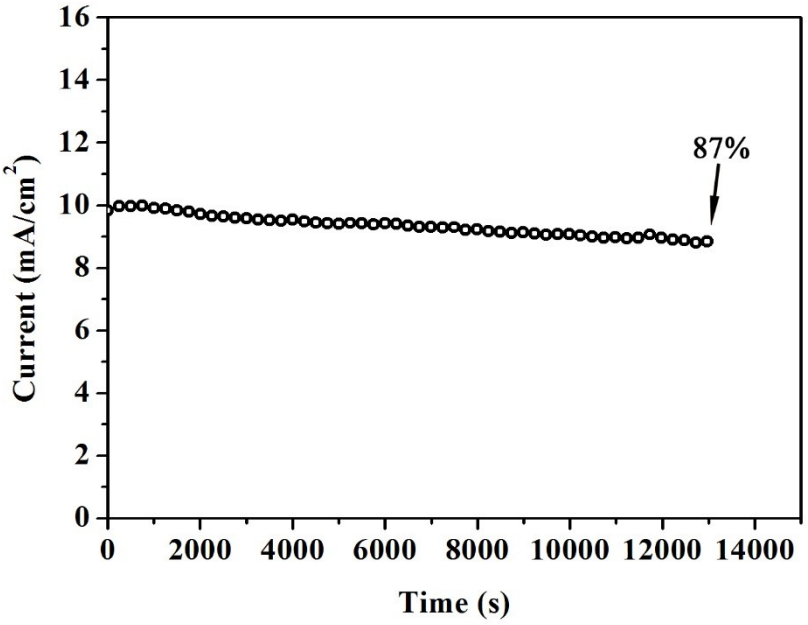

Figure. S10 I-t plot of $Co_{0.1}$@NC (without β-Mo_2C) at a controlled potential of 1.65 V.

As a comparation, the OER performance of the sample without β-Mo_2C (dubbed as $Co_{0.1}$@NC) was tested in the same condition, shown in Figure S9, revealing an OER overpotential (η_{10}) of 420 mV. $Co_{0.1}$@NC was tested for its long-term stability at 1.65 V, aiming to prove the stability brought by the existence of β-Mo_2C. As shown in Figure S10, after mere 3.6 h chronoamperometry test, the current value dropped to 87% of the initial current accompanied with a continuous decline trend, demonstrating the contribution of β-Mo_2C towards the long-term stability of the electrocatalyst.

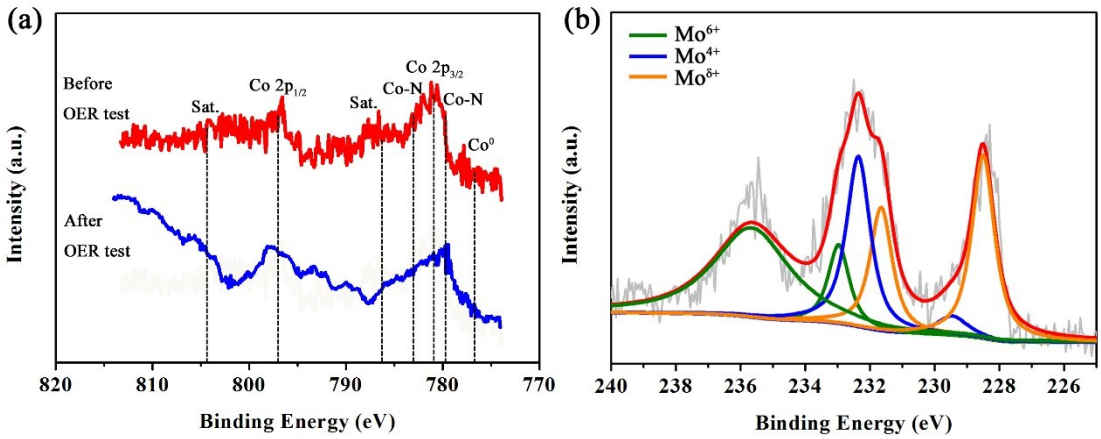

Figure. S11 XPS spectrum of $Co_{0.1}$-β-Mo_2C@NC after OER test, (a) Co and (b) Mo.

Furthermore, the XPS measurement was utilized to observe the variation of the $Co_{0.1}$-β-Mo_2C@NC after stability test. The peaks of Co-N and Co did not change in Co XPS spectrum, revealing the stability of the catalyst during the OER process (Figure S11 a)[3]. The Mo peaks of the catalyst demonstrated a phenomena of higher binding energy compared to that before test. There have been similar reports before, but the mechanism is still unknown[3, 4], as shown in Figure S11b and Table S3.

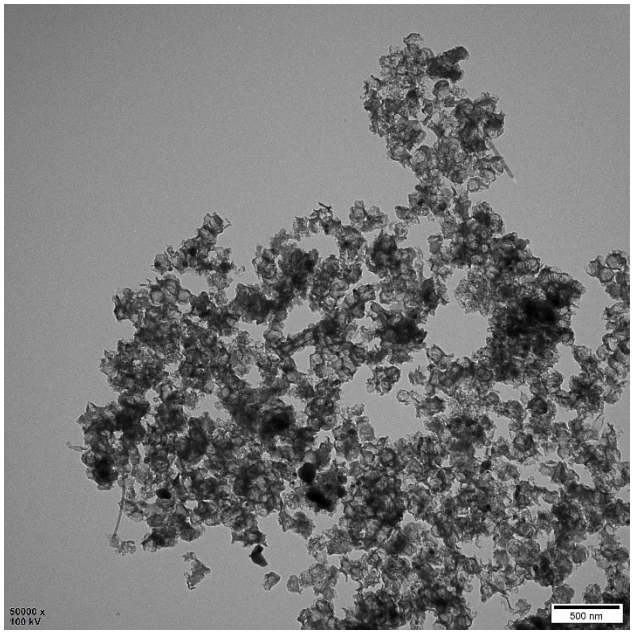

Figure. S12 TEM image of the $Co_{0.1}$-β-Mo_2C@NC after I-t test.

Table S1. Cobalt element contents (wt%) of different samples analyzed by ICP-AES.

Sample	Co/ICP (wt%)	Mo/ICP (wt%)
$Co_{0.2}$-β-Mo_2C@NC	3.91	10.89
$Co_{0.1}$-β-Mo_2C@NC	2.59	10.61
$Co_{0.05}$-β-Mo_2C@NC	1.59	10.54

Calcination step under N_2 atmosphere ensured the formation of β-Mo_2C nanoparticles, which is the effectively catalytical key factor and the complete carbonization of the carbon matrix. Moreover, cobalt content of these samples analyzed by inductively coupled plasma atomic emission spectroscopy (ICP-AES) were 3.91 wt%, 2.59 wt% and 1.59 wt%, respectively (Table S1), which indicated very low cobalt contents in materials, consisting with the XRD analysis and the theme of doping. While the exact content of Mo_2C were 5.45 wt%, 5.31 wt% and 5.27 wt%, according to ICP-AES results of Mo in these samples (10.89 wt%, 10.61 wt% and 10.54 wt%).

Table S2. Comparison of OER activity of various electrocatalysts.

Electrocatalyst	Support	η at 10 mA/cm^2 (mV)	Electrolyte	Reference
$Co_{0.1}$-β-Mo_2C@NC	**Glassy carbon**	**262.2**	**1.0 M KOH**	**This work**
Co-Mo_2C NPs	Glassy carbon	347	0.1 M KOH	[5]
Co−Mo_2C@NCNT	Glassy carbon	377	1.0 M KOH	[6]
Ni/Mo_2C-NCNFs	Glassy carbon	288	1.0 M KOH	[7]
Ni/Mo_2C-PC	Glassy carbon	368	1.0 M KOH	[8]
Co-NC@Mo_2C	Glassy carbon	347	1.0 M KOH	[9]
Co/β-Mo_2C@N-CNTs	Glassy carbon	246	1.0 M KOH	[3]
NiCo/Fe_3O_4/MOF-74	Glassy carbon	238	1.0 M KOH	[10]
Co_3O_4 nanosheets	Ti foil	300	0.1 M KOH	[11]

$CoNi(OH)_x$ nanotubes	Cu foil	280	1.0 M KOH	[12]
NiCoFeB nanochains	Glassy carbon	284	1.0 M KOH	[13]

Table S3. Comparison of the High-resolution Mo 3d XPS spectra of $Co_{0.1}$-β-Mo_2C@NC before and after cyclic test.

Sample	Mo			
		Binding Energy (eV)	Area	Percentage (%)
$Co_{0.1}$-β-Mo_2C@NC before OER	$Mo^{\delta+}$ $3d_{5/2}$	227.90	914.58	16.37
	Mo^{4+} $3d_{5/2}$	229.70	426.51	7.63
	$Mo^{\delta+}$ $3d_{3/2}$	231.20	790.74	14.15
	Mo^{4+} $3d_{3/2}$	231.90	1155.53	20.68
	Mo^{6+} $3d_{5/2}$	232.30	686.34	12.28
	Mo^{6+} $3d_{3/2}$	234.95	1613.93	28.88
$Co_{0.1}$-β-Mo_2C@NC after OER	$Mo^{\delta+}$ $3d_{5/2}$	228.50	1174.91	9.84
	Mo^{4+} $3d_{3/2}$	229.50	1028.70	8.62
	$Mo^{\delta+}$ $3d_{5/2}$	231.65	2360.03	19.77
	Mo^{4+} $3d_{3/2}$	232.35	2267.34	18.99
	Mo^{6+} $3d_{5/2}$	232.95	1342.18	11.24
	Mo^{6+} $3d_{3/2}$	235.70	3763.86	31.53

Reference:

1. Y. Z. Chen, C. Wang, Z. Y. Wu, Y. Xiong, Q. Xu, S. H. Yu and H. L. Jiang, *Adv. Mater.*, 2015, **27**, 5010-5016.
2. L. Huang, X. Zhang, Q. Wang, Y. Han, Y. Fang and S. Dong, *J. Am. Chem. Soc.*, 2018, **140**, 1142-1147.
3. T. Ouyang, Y. Q. Ye, C. Y. Wu, K. Xiao and Z. Q. Liu, *Angew. Chem., Int. Ed.*, 2019, **58**, 4923-4928.
4. J. Wang, F. Xu, H. Jin, Y. Chen and Y. Wang, *Adv. Mater.*, 2017, **29**, 1605838.
5. M. Kim, S. Kim, D. Song, S. Oh, K. J. Chang and E. Cho, *Appl. Catal., B*, 2018, **227**, 340-348.
6. L. Ai, J. Su, M. Wang and J. Jiang, *ACS Sustainable Chem. Eng.*, 2018, **6**, 9912-9920.
7. M. X. Li, Y. Zhu, H. Y. Wang, C. Wang, N. Pinna and X. F. Lu, *Adv. Energy Mater.*, 2019, **9**, 1803185.
8. Z. Y. Yu, Y. Duan, M. R. Gao, C. C. Lang, Y. R. Zheng and S. H. Yu, *Chem. Sci.*, 2017, **8**, 968-973.
9. Q. Liang, H. Jin, Z. Wang, Y. Xiong, S. Yuan, X. Zeng, D. He and S. Mu, *Nano Energy*, 2019, **57**, 746-752.
10. X. Wang, H. Xiao, A. Li, Z. Li, S. Liu, Q. Zhang, Y. Gong, L. Zheng, Y. Zhu, C. Chen, D. Wang, Q. Peng, L. Gu, X. Han, J. Li and Y. Li, *J. Am. Chem. Soc.*, 2018, **140**, 15336-15341.
11. L. Xu, Q. Jiang, Z. Xiao, X. Li, J. Huo, S. Wang and L. Dai, *Angew. Chem., Int. Ed.*, 2016, **55**, 5277-5281.
12. S. W. Li, Y. C. Wang, S. J. Peng, L. J. Zhang, A. M. Al-Enizi, H. Zhang, X. H. Sun and G. F. Zheng, *Adv. Energy Mater.*, 2016, **6**, 1501661.
13. Y. Li, B. Huang, Y. Sun, M. Luo, Y. Yang, Y. Qin, L. Wang, C. Li, F. Lv, W. Zhang and S. Guo, *Small*, 2019, **15**, 1804212.